BIOINFORMATION
Discovery at the interface of physical and biological sciences

open access www.bioinformation.net Hypothesis

Volume 6(6)

Binding mode prediction and inhibitor design of anti-influenza virus diketo acids targeting metalloenzyme RNA polymerase by molecular docking

Yoshinobu Ishikawa* & Satoshi Fujii

School of Pharmaceutical Sciences, University of Shizuoka, 52-1 Yada, Suruga-ku, Shizuoka 422-8526, Japan; Yoshinobu Ishikawa - Email: ishi206@u-shizuoka-ken.ac.jp; Phone & Fax: +81 54 264 5645; *Corresponding author

Received May 19, 2011; Accepted May 21, 2011; Published June 06, 2011

Abstract:
Influenza is a yearly seasonal threat and major cause of mortality, particularly in children and the elderly. Although neuraminidase inhibitors and M2 protein blockers are used for medication, drug resistance has gradually emerged. Thus, the development of effective anti-influenza drugs targeting different constituent proteins of the virus is urgently desired. In this light, we carried out molecular docking to predict the binding modes of anti-influenza diketo acid inhibitors in the active site of the PA_N subunit of the metalloenzyme RNA polymerase of influenza virus. The calculations suggested that the dianionic forms of the diketo acids should chelate the dinuclear manganese center as dinucleating ligands and sequester it. They also indicated that the diketo acid derivatives with larger hydrophobic substituents should block a hydrophobic cavity in the active site more tightly. These assumptions could adequately explain the enzyme inhibition by these compounds. Furthermore, we designed potential inhibitors by lead optimization of a diketo acid inhibitor from the thermodynamic points of view. Molecular docking results showed that the newly designed diketo acid derivatives might inhibit the metalloenzyme RNA polymerase more strongly than the lead inhibitor.

Keywords: Influenza, RNA polymerase, Metalloenzyme, Diketo acid, Molecular docking, Drug design

Background:
An epidemic of influenza is a yearly seasonal threat. On the other hand, the 2009 H1N1 swine flu unexpectedly ran riot around the world. It is a major cause of mortality, particularly in children and the elderly. Although several anti-influenza drugs, neuraminidase inhibitors, and M2 protein blockers are used for medication against this virus, drug resistance has gradually emerged **[1-3]**. In addition, the supply of viral vaccine is inadequate. Thus, the development of effective anti-influenza drugs targeting different constituent proteins of the virus is urgently desired **[4]**. The influenza virus is a segmented negative-stranded RNA virus. The synthesis of influenza virus mRNA occurs in the nuclei of infected cells and is catalyzed by a viral RNA polymerase consisting of the three subunits, PA, PB1, and PB2 **[5]**. This RNA-dependent enzyme possesses endonuclease and RNA transcriptase activities, and is hence essential for viral replication. Although the RNA polymerase is highly conserved among influenza A, B, and C viruses, no homologue has been found in mammalian cells **[6]**. Thus, a viral RNA polymerase is a safe target in terms of selective toxicity.

Tomassini *et al*. reported that a series of diketo acid derivatives, **1-8**, are effective inhibitors of influenza viral replication in both in vitro cell culture replication assays and in vivo mouse challenge model, without exhibiting any cytotoxicity (**Figure 1**) **[7, 8]**. Given that the action is due to the inhibition of the endonuclease activity of the viral RNA polymerase, the enzyme is currently regarded as a promising target for anti-influenza virus agents **[9]**. Recently, studies on the crystallography of the PA subunit have revealed that PA_N, the N-terminal domain of PA, contains one Mg ion or two Mn ions in the endonuclease active site **[10–12]**. The endonuclease activity of the PA_N subunit with two Mn ions is inhibited by the diketo acid derivative **5** **[12]**. This suggests that **1-8** should bind tightly to the active site of the PA_N subunit and inhibit endonuclease activity. Given that compounds **9-12**, which lack a β-diketone or carboxylic acid group, do not show inhibition of endonuclease activity, the diketo acid moiety is a pharmacophore for the anti-influenza virus activity **[13]**. In addition to the significance of the pharmacophore, it is suggested that the inhibitory activity should depend on the hydrophobicity of the aliphatic substituents. Hence, the interaction between the hydrophobic substituents and non-polar residues in the active site should be associated with enzyme inhibition.

Our objective in this study was to rationalize the inhibitory action of the diketo acid derivatives to the PA_N subunit of the metalloenzyme RNA polymerase and to design potential diketo acid inhibitors by structure-based and computer-aided modeling approach. Hence, we carried out molecular docking to predict how the anti-influenza virus diketo acid derivatives would bind to the active site of the PA_N subunit. To our knowledge, this is the first modeling study to elucidate the interaction of the PA_N subunit with anti-influenza virus diketo acid derivatives.

BIOINFORMATION open access

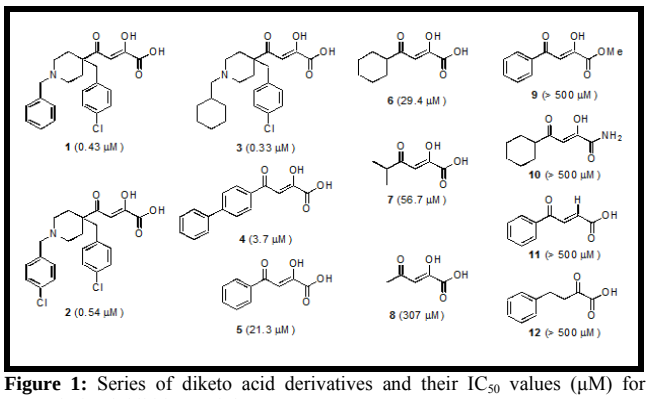

Figure 1: Series of diketo acid derivatives and their IC_{50} values (μM) for transcription inhibition activity.

Methodology:

The geometry optimization and electrostatic potential calculation of the dianionic forms of diketo acid derivatives were performed using Gaussian 03 with the B3LYP hybrid functional and the 6-31+G(d) basis set **[14]**. The restrained electrostatic potential charge fitting of the electrostatic potentials of the optimized structures was carried out with the *antechamber* module in AMBER9 **[15]**. The crystal structure (ID: 2w69, chain D) of the PA_N subunit with two Mn ions was obtained from PDB **[12]**. All water molecules and sulfate ions were stripped from the coordinates of the crystal structure, and then hydrogen atoms were added through WHATIF web server (http://swift.cmbi.ru.nl/servers/html/prepdock.html). The Gasteiger charges and +2.0 charges were assigned for the amino acids and two Mn ions, respectively. A grid of 30.0 Å x 30.0 Å x 30.0 Å with 0.375 Å spacing was calculated using AutoGrid. Automated ligand-flexible and receptor-flexible molecular docking calculations were performed and analyzed using AutoDock 4.2 and AutoDockTools **[16]**. One hundred docking runs for every compound were performed. Each docking calculation consisted of 25 million energy evaluations (long mode) using the Lamarckian genetic algorithm method. Maximum number of generations was set to 270,000. All the other parameters were set by default. The docking results were clustered on the basis of root-mean-square deviation between the Cartesian coordinates of the atoms using 2.0 Å cutoff, and were ranked on the basis of the binding free energy (BFE, kcal/mol) calculated by AutoDock 4.2.

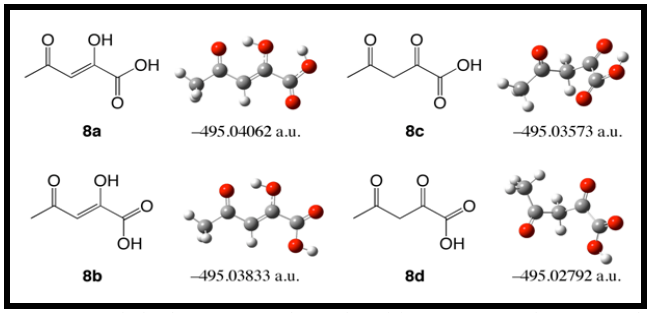

Figure 2: Optimized structures and energies of four tautomers of **8**. Gray, red, and white spheres depict carbon, oxygen, and hydrogen atoms, respectively.

Results and Discussion:

Prior to the molecular docking, we evaluated the stability of four tautomers of the simplest diketo acid **8** according to density functional theory (DFT). The geometry optimization of the tautomers was carried out with the B3LYP hybrid functional and 6-31G(d) basis set **[14]**. As shown in **Figure 2**, the optimized structures and energies indicated that the enol forms **8a** (E = –495.04062 a.u.) and **8b** (E = –495.03833 a.u.) were more stable than the keto forms **8c** (E = –495.03573 a.u.) and **8d** (E = –495.02792 a.u.). Furthermore, the enol form with an intramolecular hydrogen bond between the enol and carboxylic acid groups (**8a**) was more stable than the one without the intramolecular hydrogen bond (**8b**). As a result, **8a** was the most stable tautomer, suggesting that its population is the highest. Given the p*K*a of the terminal carboxylic acid of diketo acids (p*K*a ~ 4) **[17]**, potential chelating ability of the β-diketone group, structure-activity relationship, and DFT results, it is the dianionic forms of diketo acid derivatives that should readily coordinate with the two Mn ions in the active site of the PA_N subunit, as shown in **Figure 3**. The driving forces of the interaction are likely to be the chelate effect, enthalpically favorable electrostatic interaction between the Mn^{2+} and oxo ions, and the entropically favorable release of water molecules generated by the acid-base reaction of the diketo acids with the coordinated hydroxo bases. Sequestering the metal ions should disturb the access of the substrate, and thus inhibit enzyme function **[18]**. In addition, the hydrophobic interaction between the substituents of the diketo acid derivatives and the residues in the active site should be systematically related to the affinities and inhibitory activities of the diketo acid derivatives. Hence, we predicted the binding modes of the dianionic forms of the diketo acid derivatives in the active site of the PA_N subunit having two Mn ions.

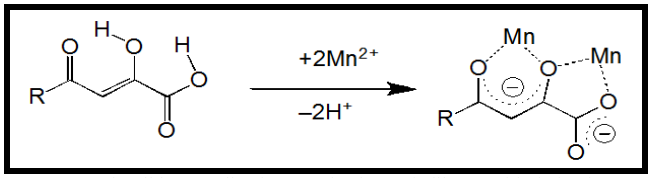

Figure 3: Plausible coordination mechanism of diketo acid derivatives to dinuclear Mn center in active site of PA_N subunit of influenza RNA polymerase.

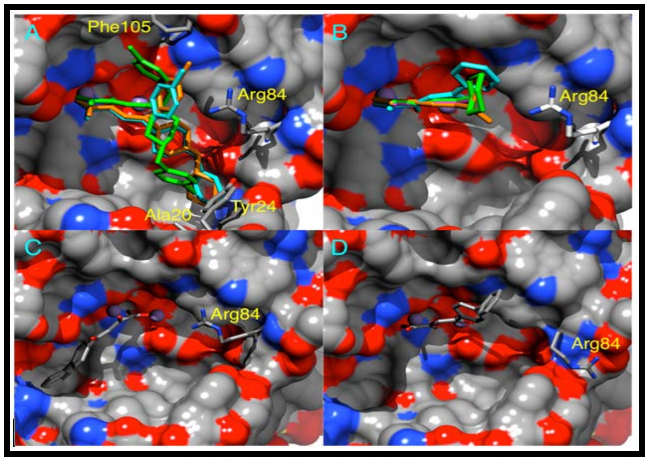

Figure 4: (A) Top-ranked flexible-ligand and rigid-receptor docking poses of **1** (cyan), **2** (green), and **3** (orange); **(B)** Top-ranked flexible-ligand and rigid-receptor docking poses of **5** (cyan), **6** (green), **7** (orange), and **8** (purple); **(C)** Top-ranked flexible-ligand and rigid-receptor docking pose of **4**; **(D)** Flexible-ligand and flexible-Arg84 docking pose of **4**.

The top-ranked docking poses for compound **1-3** and **5-8** in terms of flexible-ligand and rigid-receptor docking are shown in **Figures 4A & 4B**, respectively, and their BFEs are listed in **Table 1 (see Supplementary material)**. As expected, the dianionic moieties were predicted to chelate the dinuclear Mn center as dinucleating ligands. For **1-3**, the chlorobenzyl groups were exposed on the outside of the active site, and they had contact with Phe105 and Arg84 at the edge. On the other hand, the aryl/cyclohexyl piperidine substituents were in a deeper position, and they had van der Waals contacts with Tyr24 and Ala20. The burial of the hydrophobic groups upon binding should result in desolvation entropy gain because of the release of water molecules into the bulk solution. No hydrogen bond was seen for the piperidine nitrogens. Thus, the right side of the active site was blocked by chelation and hydrophobic interaction, both of which should contribute to higher inhibitory effect. The poorer inhibitory effect for **5-8** is most likely due to the lack of aliphatic substituents that interact hydrophobically with any amino acid residue in the deeper position. The top-ranked docking pose for **4** was different from that for the others mentioned above. The only carboxylate group coordinated to and bridged two Mn ions, and the biphenyl substituent interacted with a hydrophobic pocket on the left side (**Figure 4C**). However, diketo acid **4** need not be of diketonate form in this docking pose, and thus its BFE is overestimated. This unexpected improper docking result could arise from steric hindrance between Arg84 and the biphenyl substituent. Thus, a molecular docking taking into account the flexibility of Arg84 was carried out. There was space to pack the Arg84 residue, and steric hindrance was avoided by the inversion of the Arg84 residue. This resulted in the chelation by the dianionic form of **4** as the dinucleating ligand, as shown in **Figure 4D**.

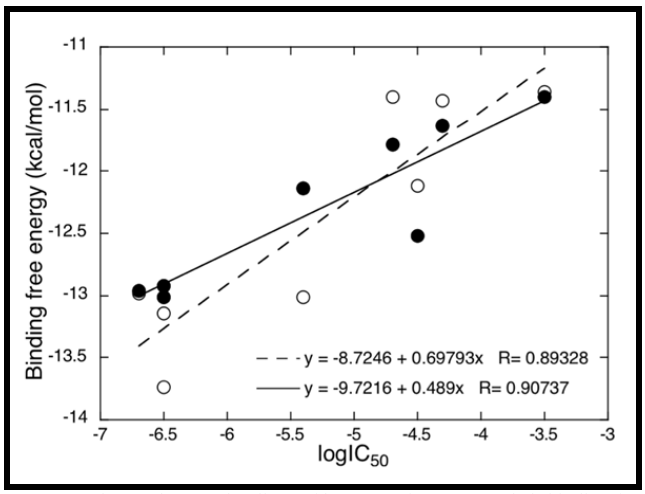

Figure 5: Plots and regression lines of $logIC_{50}$s of **1-8** versus their binding free energies with rigid-receptor (open circles and dashed line) and flexible-Arg84 receptor (filled circles and solid line) models.

In the light of the flexibility of Arg84, molecular docking calculations were also performed for the other diketo acid derivatives. The $logIC_{50}$ values for transcription inhibition activity and the BFEs of **1-8** when using a flexible-Arg84 receptor model are listed in **Table 1**. The plots of the $logIC_{50}$s and BFEs shown in **Figure 5** reveal that the $logIC_{50}$s of **1-8** are well correlated with the corresponding BFEs. In particular, it is noted that the correlation in the case of flexible-Arg84 dockings (R = 0.91) was superior to that in the case of rigid-receptor dockings (R = 0.89). In addition, molecular docking calculations including the flexibilities of Arg84 and the residues adjacent to Arg84 were also performed to test if the correlation could be improved by using a receptor model with two or three flexible residues. The correlations resulting from flexible-Arg84-Tyr24 (R = 0.79) and flexible-Arg84-Tyr24-Trp88 dockings (R = 0.64) were lower than those resulting from the rigid-receptor and flexible-Arg84 dockings (**Figure S1, see Supplementary material**). This suggests that Arg84 is a key residue in predicting the binding mode.

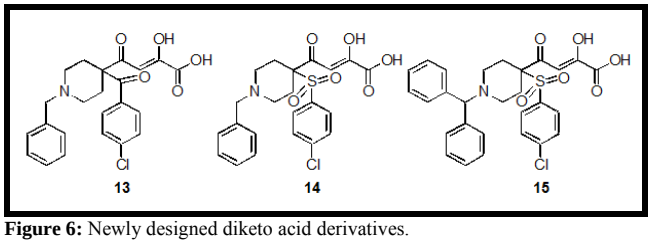

Figure 6: Newly designed diketo acid derivatives.

On the basis of our predicted binding models, we propose potential diketo acid inhibitors **13-15**, as shown in **Figure 6**, by lead optimization of **1**. Chemical functionalities were introduced from the viewpoint of enthalpy and entropy of binding, which determine the Gibbs energy of binding (i.e., binding affinity). The introduction of a hydrogen bond donor/acceptor to establish favorable enthalpic interaction with the target was considered. **Figure 7A** shows the flexible-Arg84 docking pose of **1**. It was found that the proton donor residue Arg84 was conveniently close to the chlorobenzyl piperidine moiety. This suggested that the replacement of the methylene group with a carbonyl group as a proton acceptor might result in a favorable hydrogen bond. The top-ranked docking pose of **13** with the flexible-Arg84 receptor showed a hydrogen bond between its carbonyl group and Arg84 (**Figure 7B**). The introduction of the carbonyl group lowers the BFE of flexible-Arg84 docking in **13** (–13.31 kcal/mol) relative to that in **1** (–12.92 kcal/mol). Furthermore, it was inferred that replacement of the carbonyl group with a sulfonyl group could result in a more favorable hydrogen bond. The top-ranked rigid-receptor and flexible-Arg84 docking poses of **14** are shown in **Figures 7C** and **7D**, respectively. The docking pose of **14** with the flexible-Arg84 receptor also showed a hydrogen bond between its sulfonyl group and Arg84. The BFE of flexible-Arg84 docking in **14** was lower (–14.21 kcal/mol) than that in **13**, suggesting that in the docking models, the sulfonyl group might be better than the carbonyl group as the hydrogen acceptor with higher affinity. Entropic optimization by increasing hydrophobicity was derived by the careful visual inspection of the docking results. From a comparison of the top-ranked docking pose (BFE = –13.23 kcal/mol, **Figure 7C**) of **14** with the second top-ranked pose (BFE = –13.22 kcal/mol, **Figure 8A**) when using the rigid-receptor model, we found that there was room for packing an additional phenyl ring in the deep cavity. Thus, compound **15** was designed by introducing a diphenylmethyl group, commonly found in marketed drugs, in place of the benzyl group. The top-ranked rigid-receptor (BFE = –14.39 kcal/mol) and flexible-Arg84 docking poses (BFE = –14.90 kcal/mol) of **15** are shown in **Figures 8B** and **8C**, respectively. The docking pose of **15** when using the flexible-Arg84 receptor model exhibited a hydrogen bond between its sulfonyl group and Arg84, as well as a hydrophobic contact of the diphenylmethyl group in the deep cavity. Few conformational differences were observed between the top-ranked rigid-receptor and flexible-Arg84 docking poses of **15** and between the poses of their corresponding Arg84 residues. This suggests the adequacy of the positions for the introduction of the hydrogen bond acceptor and the hydrophobic substituent. As a result, the BFEs of **15** demonstrated the highest affinities among all the diketo acid derivatives when using both the rigid-receptor and flexible-Arg84 receptor models. The inhibitory activity of **15** might increase by a few orders of magnitude relative to that of **1**, as estimated by the linear regression model in **Figure 5**.

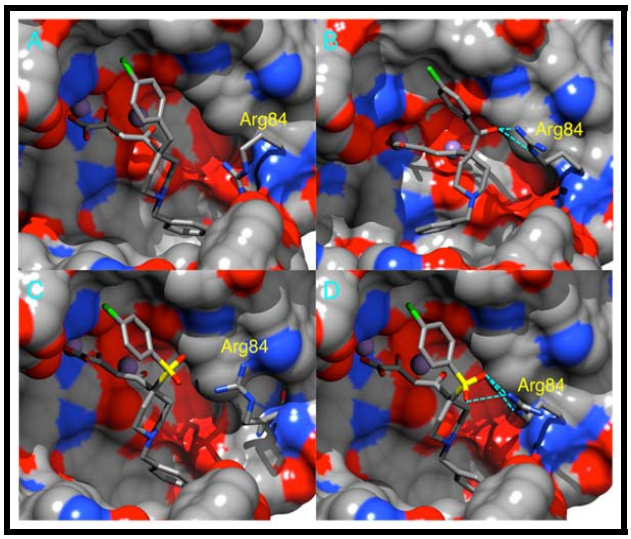

Figure 7: (A) Top-ranked flexible-ligand and flexible-Arg84 docking pose of **1**; **(B)** Top-ranked flexible-ligand and flexible-Arg84 docking pose of **13**; **(C)** Top-ranked flexible-ligand and rigid-receptor docking pose of **14**; **(D)** Top-ranked flexible-ligand and flexible-Arg84 docking pose of **14**.

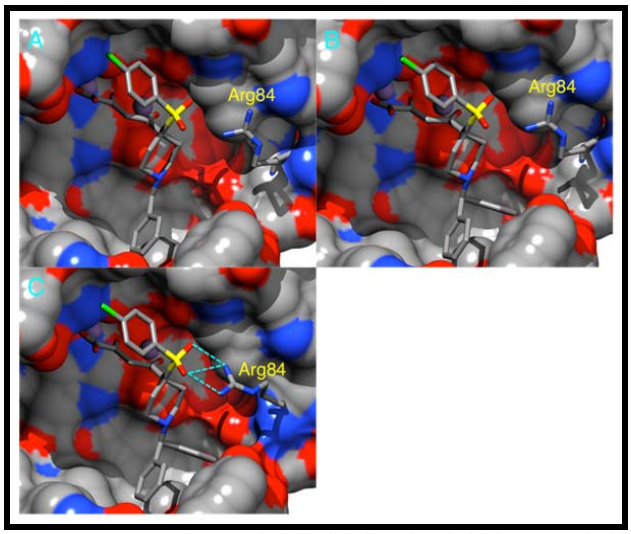

Figure 8: (A) Second top-ranked flexible-ligand and rigid-receptor docking pose of **14**; **(B)** Top-ranked flexible-ligand and rigid-receptor docking pose of **15**; **(C)** Top-ranked flexible-ligand and flexible-Arg84 docking pose of **15**.

Conclusion:

In this work, we proposed the binding mode of anti-influenza diketo acid derivatives in the active site of the PA_N subunit of the RNA polymerase, of the influenza virus, by molecular docking. The calculations suggested that the dianionic forms, of the diketo acids, should chelate the dinuclear Mn center as dinucleating ligands and sequester it. In addition, they indicated that the aliphatic substituents of the diketo acid derivatives should properly block the hydrophobic cavity in the active site, and thus inhibit endonuclease activity. The accuracy of the predicted binding modes was validated by the excellent correlation between the $logIC_{50}$s of the diketo acid derivatives and the corresponding BFEs. Potential diketo acid inhibitors were designed from the thermodynamic point of view by structure-guided and computer-assisted modeling approach. The critical residue for the lead optimization of diketo acid derivatives is likely to be the proton donor Arg84. The molecular docking results showed that the newly designed diketo acid derivatives with the proton acceptor of a carbonyl or sulfonyl group might inhibit the metalloenzyme RNA polymerase more strongly than the lead compound. We hope that our study can contribute to the development of potent influenza virus inhibitors targeting the RNA polymerase, which is essential for viral replication.

References:

[1] Carr J *et al*. *Antiviral Res*. 2002 **54**: 79 [PMID: 12062393]
[2] Herlocher ML *et al*. *Antiviral Res*. 2002 **54**: 99 [PMID: 12062395]
[3] Cheer SM & Wagstaff AJ. *Am J Respir Med.* 2002 **1**: 147 [PMID: 14720068]
[4] Das K *et al*. *Nat Struct Mol Biol.* 2010 **17**: 530 [PMID: 20383144]
[5] Liu Y *et al*. *Sci China C Life Sci*. 2009 **52**: 450 [PMID: 19471867]
[6] Yamashita M *et al*. *Virology.* 1989 **171**: 458 [PMID: 2763462]
[7] Tomassini J *et al*. *Antimicrob Agents Chemother*. 1994 **38**: 2827 [PMID: 7695269]
[8] Hastings JC *et al*. *Antimicrob Agents Chemother*. 1996 **40**: 1304 [PMID: 8723491]
[9] Nakazawa M *et al*. *Antiviral Res*. 2008 **78**: 194 [PMID: 18258312]
[10] Yuan P *et al*. *Nature* 2009 **458**: 909 [PMID: 19194458]
[11] Zhao C *et al*. *J Virol*. 2009 **83**: 9024 [PMID: 19587036]
[12] Dias A *et al*. *Nature* 2009 **458**: 914 [PMID: 19194459]
[13] Parkes KE *et al*. *J Med Chem.* 2003 **46**: 1153 [PMID: 12646026]
[14] http://www.gaussian.com/g_misc/g03/citation_g03.htm
[15] Wang J *et al*. *J Mol Graph Model*. 2006 **25**: 247 [PMID: 16458552]
[16] Morris GM *et al*. *J Comput Chem*. 2009 **30**: 2785 [PMID: 19399780]
[17] Sechi M *et al*. *J Med Chem*. 2006 **49**: 4248 [PMID: 16821784]
[18] Kirschberg T & Parrish J. *J Curr Opin Drug Discov Devel*. 2007 **10**: 460 [PMID: 17659488]

Edited by P Kangueane
Citation: Ishikawa & Fujii. Bioinformation 6(6): 221-225 (2011)

BIOINFORMATION

open access

Supplementary material:

Table 1: The $logIC_{50}$s and calculated BFEs with rigid-receptor and flexible-Arg84 receptor models for the diketo acid derivatives.

Compds	$logIC_{50}$[a]	BFE in rigid receptor, kcal/mol	BFE in flexible-R84 receptor, kcal/mol
1	–6.5	–13.14	–12.92
2	–6.7	–12.98	–12.96
3	–6.5	–13.74	–13.01
4	–5.4	–13.01	–12.14
5	–4.7	–11.40	–11.78
6	–4.5	–12.12	–12.52
7	–4.3	–11.43	–11.63
8	–3.5	–11.36	–11.40
13		–12.96	–13.31
14		–13.23	–14.21
15		–14.39	–14.90

[a]Ref. **[7]**.

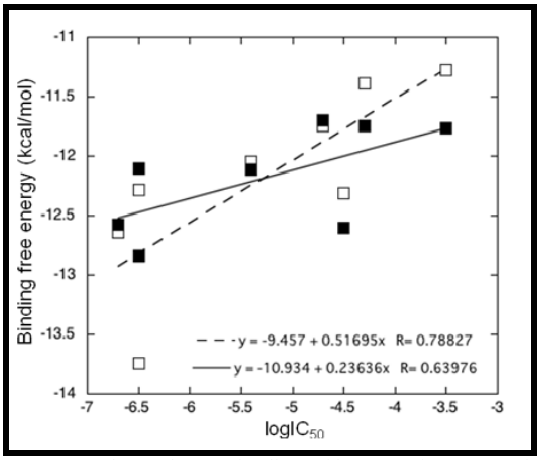

Figure S1: Plots and regression lines of $logIC_{50}$s of **1-8** versus their binding free energies with flexible-Arg84-Tyr24 receptor (open squares and dashed line) and flexible-Arg84-Tyr24-Trp88 receptor (filled squares and solid line) models.